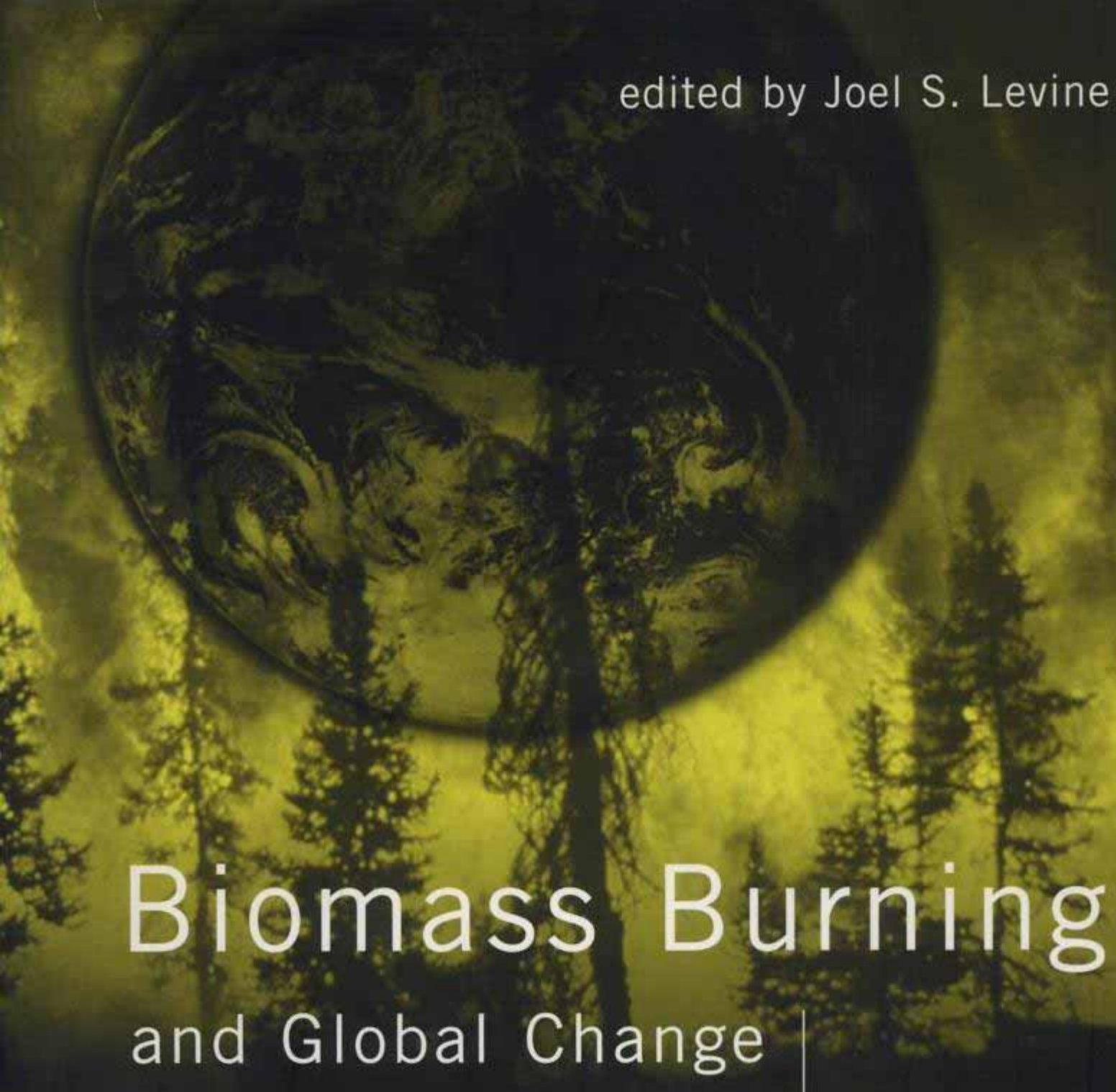
edited by Joel S. Levine
Biomass Burning
and Global Change

This book was set in Times Roman on the Monotype "Prism Plus" PostScript Imagesetter by Asco Trade Typesetting Ltd., Hong Kong.
Editorial and production services were provided by Superscript Editorial Production Services.
Printed and bound in the United States of America.

Library of Congress Cataloging-in-Publication Data

Biomass burning and global change / edited by Joel S. Levine.
p. cm.
Includes bibliographical references and index.
ISBN 0-262-12201-4 (vol. 1 : alk. paper). —
ISBN 0-262-12202-2 (vol. 2 : alk. paper)
1. Burning of land—Environmental aspects.
2. Fuelwood—Burning—Environmental aspects.
3. Climatic changes. I. Levine, Joel S.
TD195.B56858 1996
628.5'3—dc20 96-35030
CIP

Temporal and Spatial Variability of Aerosol Loading and Properties during the Amazon, North American Temperate, and Boreal Forest Burning Seasons

Brent N. Holben, Thomas F. Eck, Alberto Setzer, Ilya Slutsker, Alfredo Pereira, Brian Markham, and John Vande Castle

Biomass burning plays a significant part in the major terrestrial ecosystems of the globe and recently has become the focus for study on the influence of global climate forcing through direct and indirect impacts on the radiation regime. The concentrations and properties of aerosols contribute significantly to climate radiative forcing. Hansen and Lacis (1990) state that "Aerosols are the source of our greatest uncertainty about climate forcing. Tropospheric aerosols are difficult to monitor because of their spatial inhomogeneity, but they are a crucial variable because of the strong anthropogenic influence on their amount." Additionally, modeling by Charlson et al. (1992), Penner et al. (1992, 1994) suggests that the direct and indirect radiative effects of sulfate and other aerosols in the troposphere, including those from biomass burning, may be sufficient worldwide to offset the radiative effects of increases in greenhouse gases. Penner et al. (1994) propose that synoptic-to-global-scale observations be made of the radiation budget, as well as both the composition of the aerosols and their interactions with water vapor.

Quantitative measurements are relatively sparse, discontinuous, and more likely to be found in developed regions of the world. Crutzen and Andrea (1990) estimate that 80% of the aerosol emissions from biomass burning originate in the poorly monitored tropics, thus exacerbating our ability to understand their influence on climate forcing, remote sensing, ecosystem dynamics, and health.

In the tropics, savanna burning is part of the natural ecology. Since mechanized clearing began, conversion of the tropical forests to agricultural uses has made these areas a major source of carbon and particulates emitted to the atmosphere. Recent studies show that the tropical forests have become a source of carbonaceous aerosols from biomass burning, and when combined with savanna regions, may represent about 80% of the global total (Crutzen and Andreae 1990). Biomass burning is a natural phenomenon of the savannas and cerrados, but with mechanized clearing practices and the resources required by a growing population, biomass burning has expanded rapidly over large areas of both cerrado and the tropical forests, particularly in Brazil. This expansion is shown as an increase in deforestation from 1978 to 1988 in Brazil's "Legal Amazon" from ~2% to ~6% in a decade (Skole and Tucker 1993). Fires and emissions from biomass burning have been well documented in Brazil in a variety of ways. Setzer and Pereira (1991) have monitored the number of fires in Brazil with NOAA AVHRR thermal bands since 1987. Their studies show the number of fires in the Amazon region is generally increasing but varies from year to year depending on meteorology and changing economic conditions. The primary fire season is most of August and September, with about 300 000 fires per season being typical (Setzer and Pereira 1991). Prins and Menzel (1992, 1994) have used the GOES VAS to monitor fires and the transport of aerosols to the Atlantic Ocean. In Brazil, Artaxo et al. (1994) measured in situ ground-level aerosol size distributions and mass concentrations for varying periods at a cerrado site, a forest site with biomass burning, and a background forest site. Their results clearly show an increase of 5 to 8 times in aerosol mass concentration during the burning season in August and September.

Wildfires are a part of the boreal landscape processes; their remote location and minimal impact on human habitation, compared to mid- and tropical latitudes, result in many of these fires burning themselves out almost unnoticed (Stocks 1991). Thus, their quantification of aerosol emissions has received little attention, though they represent 12×10^6 km^2 in North America and Eurasia, or approximately 25% of the world's forests. The 1987 fires in Northern China and Siberia are among the few well-documented examples of the areal extent of these fires. Using satellite estimates of burn scars, Cahoon et al. (1991) report approximately 14.4 million hectares (ha) were burned, or about 1% of the total boreal forest.

Finally, the mid-latitude forests in North America are highly managed including fire suppression and prescribed burns. Concerns over timber production,

public use, and air quality have limited the number and size of wildfire burns in most years, contributing to an accumulation of fuel that periodically leads to very large and intense wildfires that may exceed human fire-suppression capability. The result is a relatively extensive source of particulate emissions to the atmosphere.

Following is our initial documentation of the aerosol emissions and properties from parts of these three forest biomes, all principal emitters biomass burning. The longer record and more extensive areal coverage lead us to emphasize the Amazon measurements.

The Amazon Basin is a 5×10^6 km^2 region that is primarily forest, interspersed with cerrado (savanna) situated on flood plains, and plateaus and mountains that are a significant source of aerosols, gases, and water vapor to the global atmosphere (Harriss et al. 1990). Tropical forest regions are a principal source of biogenic aerosols (Cachier et al. 1985), and some measurements of these aerosols have been reported (Lawson and Winchester 1979; Artaxo and Orsini 1986; Artaxo et al. 1988, 1990, 1993, and 1994).

Beginning in 1992, an effort was mounted to measure aerosol concentration and properties from biomass burning during the southern Amazon dry season and to a limited extent during part of the wet season. Following is an assessment of the data collected to date, emphasizing the temporal characterization of the spectral aerosol optical thickness, size distribution, and precipitable water for the eight measurement sites in Brazil's Amazon Basin. In 1994 a similar network was established in boreal forests in north-central Canada, associated with the NASA-sponsored BOREAS experiment. A network of instruments was established in 1994 in the western United States forests and agricultural lands, which measured emissions from some of the large fires during that year. One of these stations is expected to be a multiyear activity associated with the Long Term Ecological Research (LTER) activities of the H. J. Andrews Experimental Forest in the central Oregon Cascades.

Spectral Scanning Radiometer Measurements

Instrument Description

The automatic sun/sky scanning spectral radiometers measured aerosol concentrations and properties from direct sun measurements at 340, 440, 670, 870, 940, and 1020 nm every 15 min. and sky radiance measurements at 440, 670, 870, and 1020 nm hourly, weather permitting. The NOAA Data Collection System geostationary satellite link transmitted the data to Wallops Island, Virginia for near real-time processing into spectral aerosol optical thickness, wavelength exponent, precipitable water, and aureole and sky radiances. Further details about the instrument specifications and data processing are given in Holben et al. (1996).

The sky radiance almucantar (measurements in a plane with a fixed-view zenith angle that includes the sun) and principal plane (measurements in a plane with a fixed-view azimuth angle that includes the sun) measurements are made hourly throughout the day at small angles through the solar aureole, and at increasingly larger angles as the scattering angle increases. These data are inverted into phase function, size distribution, and aerosol optical thickness (Nakajima 1986), using the first 40° from the solar disk. The inversion scheme continues to be developed (Nakajima 1995), but sensitivity studies show that size-distribution retrievals are reasonable between 0.1 and 4 μm (Kaufman et al. 1992, Remer et al. 1995).

Site Descriptions

The Amazon The sites were chosen to be representative of regional conditions, to capture the southerly transport of aerosols out of the Amazon basin, and to meet the logistical constraints for instrument maintenance and security. The data presented here were collected at three cerrado sites (Brasilia Lat. 16°S, Long. 49°W; Porto Nacional Lat. 10°S, Long. 48°W; Cuiaba Lat. 16°S, Long. 55°W); where burning is a natural part of the landscape processes but is augmented by increased agricultural burning and presumably by advection from forest burning. Five diverse forest sites were monitored in the eastern and southern Amazon basin (Alta Floresta Lat. 10°S, Long. 55°W; Jamari Lat. 9°S, Long. 62°W; Ji-Parana Lat. 12°S, Long. 60°W; Tucurui Lat. 4°S, Long. 48°W; and Santarem Lat. 1°S, Long. 55°W). Burning at these sites is a recent phenomenon of forest conversion, and emissions are from primary and secondary forest-fire sources. All cerrado sites have a dry season, extending on average from May through September, and in forested sites slightly shorter (Nimer 1989).

The Boreal Forests The BOREAS network is a SW to NE 600 km transect of five instruments from Prince Albert, Saskatchewan (53°N, 106°W) to Thompson, Manitoba (56°N, 98°W), all within undisturbed tracts of boreal forest. Prince Albert borders the agricultural lands to the south and Thompson the tundra to the north, encompassing much of the cover types within a boreal forest. A sixth instrument is in Bonanza Creek,

Alaska (65°N, 148°W), and is part of the LTER network.

The Temperate Forests Instruments in the temperate forest regions have been largely short-term and associated with individual field campaigns. The LTER instrument in the U.S. Forest Service H. J. Andrews Experimental Forest (44°N, 122°W) is the exception. Ukiah, Oregon (44.5°N, 119°W), and Pullman, Washington (47°N, 117°W), were placed for measuring aerosols from temperate forest fires.

Seasonal Measurements

The Amazon Most of the Amazon Basin is climatologically distinguished by a wet and dry season (Nimer 1989). However, with respect to aerosols, the dry season is clearly marked by a nonburning and burning season for all sites along the southern and eastern forest margin; the duration of each varies by location and is caused by intraseasonal variations in weather patterns. The data from the sun/sky spectral radiometer network clearly show the profound influence of biomass burning on the aerosol regime during the burning season (figure 60.1). For all sites but Santarem and Tucurui, August and September show very heavy aerosol loading, followed by a sharp decrease in October and the onset of the rains and the wet season. Preceding the burning season is a dry season, with very clear, clean air. A dramatic illustration occurs in Cuiaba in the cerrado region. Beginning in June 1993, AOT measurements were made through February 1994 that incorporated most of the dry season and several months in the wet season (figure 60.2*a*). Two features stand out: first is a very high density of measurements from June to early October (the dry season), and relatively few points from October to February (the wet season), because persistent cloud cover prevents measurements from being taken; second, an order-of-magnitude increase in AOT begins late in July and persists until early in October. This is the anthropogenic seasonality, caused by biomass burning in the region.

The spectral optical thickness is used to compute the ngstrom wavelength exponent (alpha) and is defined as:

$$\alpha = -\ln(\mathrm{AOT1}/\mathrm{AOT2})/\ln(\lambda 2/\lambda 1). \qquad (60.1)$$

Holben et al. (1991) and Kaufman et al. (1992) show that the wavelength exponent is sensitive to rapid aging of fresh smoke from fires in Brazil, estimating the effective geometric radius from 0.15 for smoke less than 10 min. old to 0.20 for smoke more than 1 day old. Many other investigators have related the wavelength exponent to the mean particle size. The seasonal distribution of the wavelength exponent shows an increase in value coinciding with the burning season (figure 60.2*b*), indicating that the proportion of particulate emissions is shifted toward smaller size distributions during the burning season. Precipitable water is measured by the instrument, which has a nominal absolute accuracy of ± 0.3 cm (Halthore et al. 1996). The seasonal dependence for Cuiaba shows an increase in Pw through the dry season, and that the Pw content in September is similar to the wet-season values and is about 70% higher than the early burning-season values (figure 60.2*c*).

The size distributions were retrieved from inversion of the daily spectral almucantar measurements made between an optical airmass of 5 and 2. The seasonal plot clearly shows the increase in the accumulation and coarse particle modes which overwhelms the constant Pinatubo mode (centered near 0.5 μm) during August and September 1993 (figure 60.3).

These data indicate that the current aerosol climatology of the Amazon region should be partitioned beyond the simple climatological limits of the wet and dry seasons. For regions with active biomass burning, we have subdivided the dry season into a preburning season, a transition-to-burning season, burning season, and transition-to-wet season. These categories are relatively subjective in their boundaries, but we have defined them by the magnitude and temporal variability of the average aerosol optical thickness at 440 nm (AOT_{440}). For example, the average AOT_{440} during the preburning season remained below 0.4 and has a standard deviation of less than 0.04. The transition-to-burning season had an average AOT_{440} ranging between 0.4 and 1.0, the burning season greater than 1.0, the transition-to-wet again between 1.0 and 0.4, and the wet season less than 0.4. The lack of data in the wet season and early preburning season due to persistent cloud cover limits our ability to characterize these seasons well, but we believe that because the Amazon Basin has few sources of anthropogenic aerosols during these periods, our limited measurements characterize the aerosol environment fairly well during that time.

These measurements cannot and were not intended to represent emissions over the entire Amazon region, but they do characterize the optical properties of aerosols and give an indication of the magnitude, variability, and duration within the region surrounding each site.

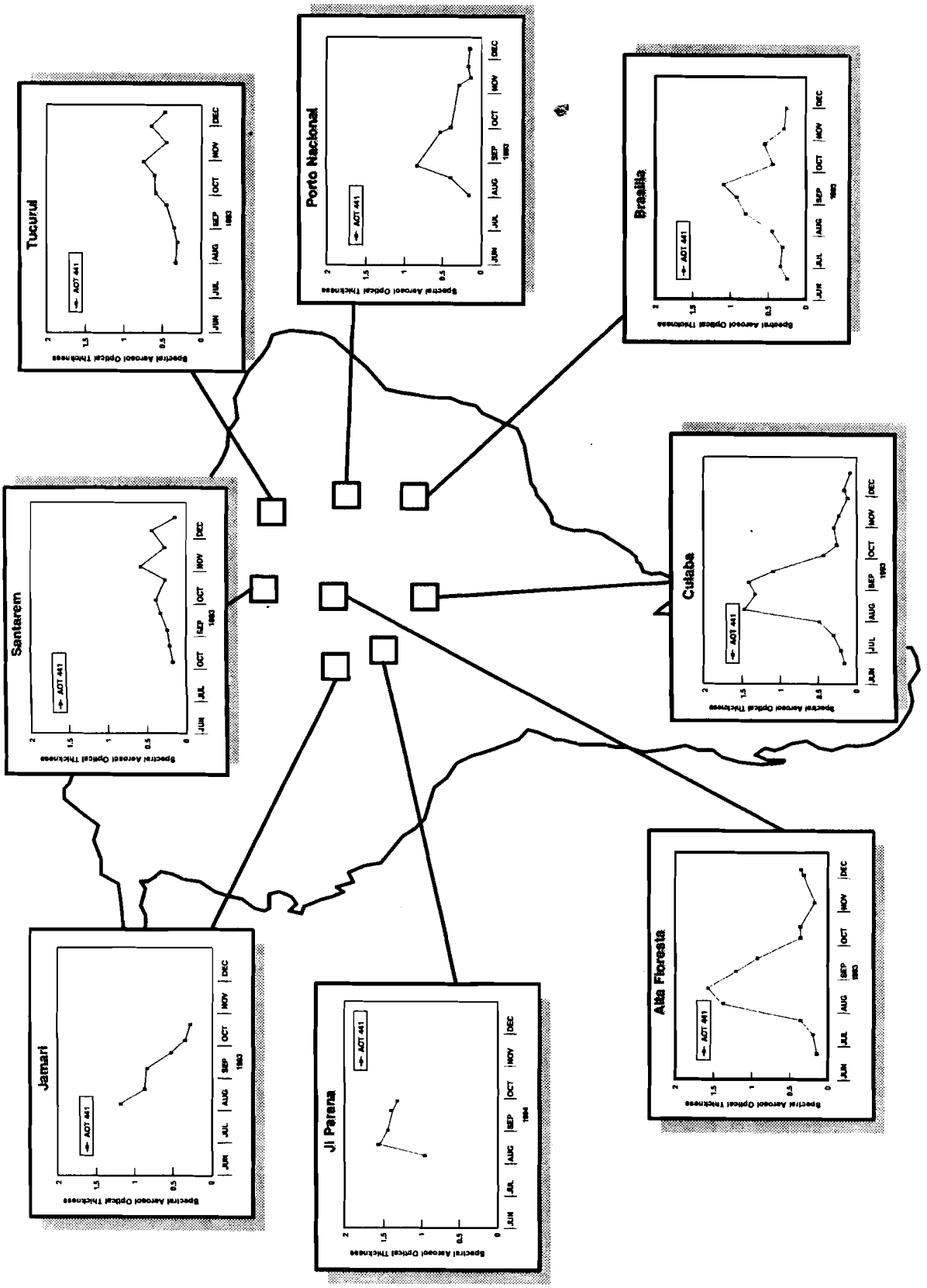

Figure 60.1 The AOT440 averaged and plotted against date clearly shows the elevated levels of aerosols to be in the southern, eastern, and western portions of Brazil's Amazon Basin. This reading corresponds to the biomass burning activities in those regions.

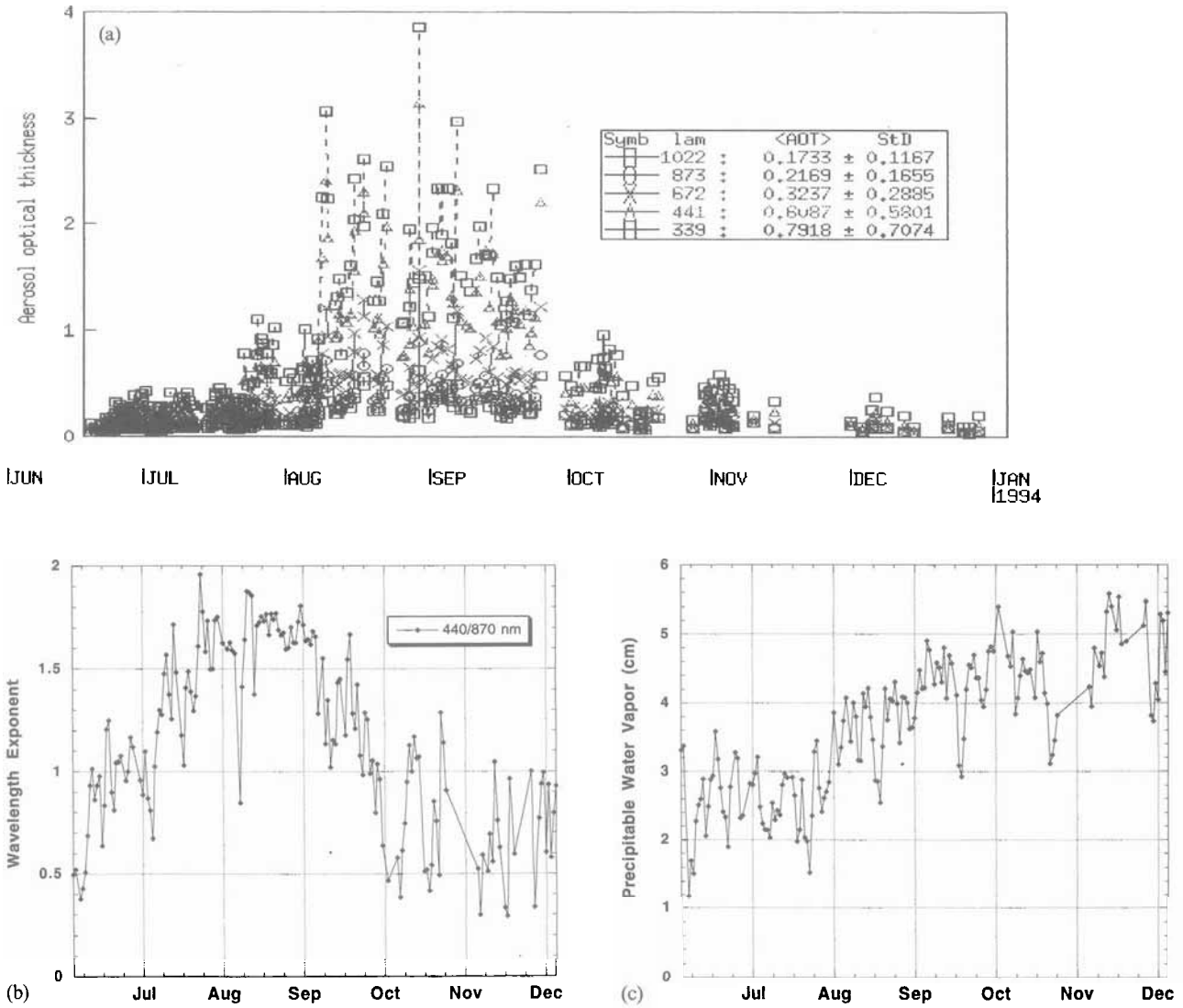

Figure 60.2 Time-dependent plots of the 1993 direct sun measurements from the spectral scanning radiometer data from Cuiaba show the seasonality for (*a*) aerosol optical thickness in five spectral bands, (*b*) the daily averaged Ångstrom wavelength exponent for the 440/870 AOT ratio, and (*c*) the daily averaged precipitable water, in cm.

The Boreal Forest The seasonal trace of aerosol optical thickness from the Thompson site is typical for all the BOREAS sites. The optical depth is low during most of the summer season, but very large spikes of several days to weeks occur in response to wildfires in the region (figure 60.4). During nonburning events, the AOT ranges from 0.1 to 0.4 at 440 nm, and during burning events, the AOT may exceed 2. for short periods. The timing of the burning events is locally dependent on occurrence of lightning strikes and fuel dryness. Two seasons of measurements show that fire occurs from early May through September. The onset of cool weather and rains can quickly reduce the potential for extensive burning.

Temperate Forests The aerosol optical thickness record for the summer dry season in the Pacific northwest indicated very light aerosol loading throughout the period for all measurement sites, despite the larger-than-average number of fires burning in the region. The HJA record shows background levels of AOT early in July (0.08 @ 440 nm), increasing to ~0.3 through August (figure 60.5). A fairly large increase occurred briefly in mid-September in response to a local fire. The data indicate that there are rarely enough fires and

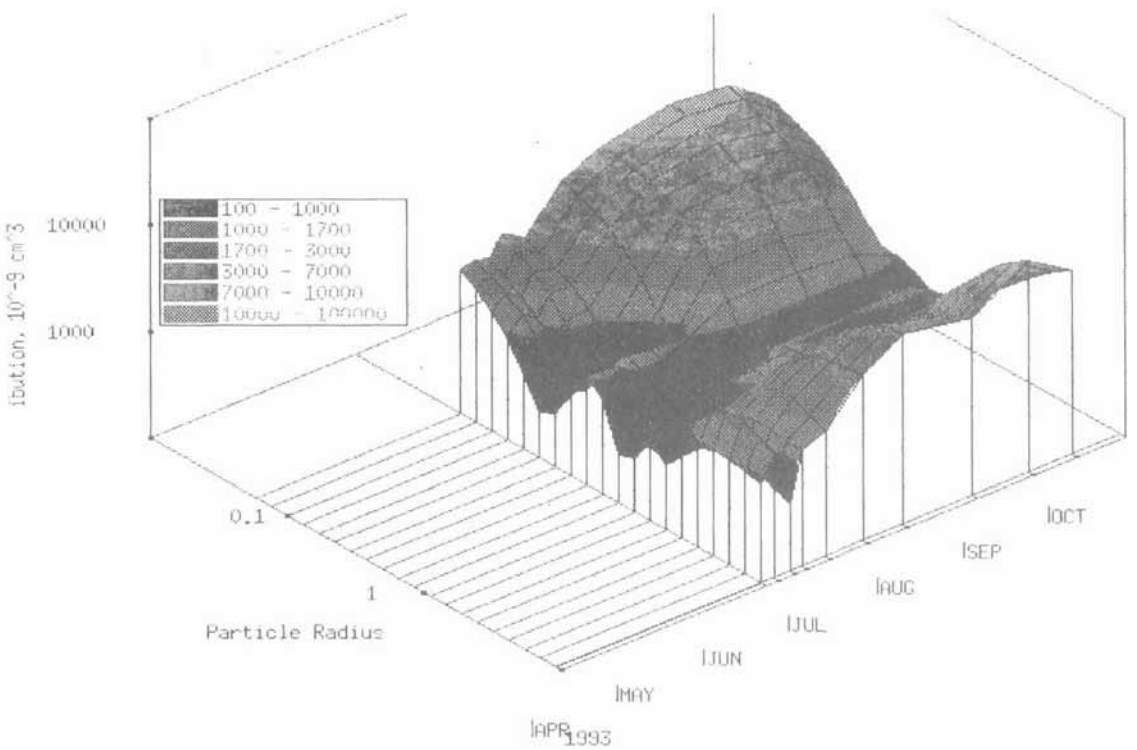

Figure 60.3 The almucantar radiance data were inverted to averaged aerosol size distributions for the clear, transition, and smoke seasons. Notice that the size distribution has peak values in the accumulation and coarse-particle modes during peak burning season in September.

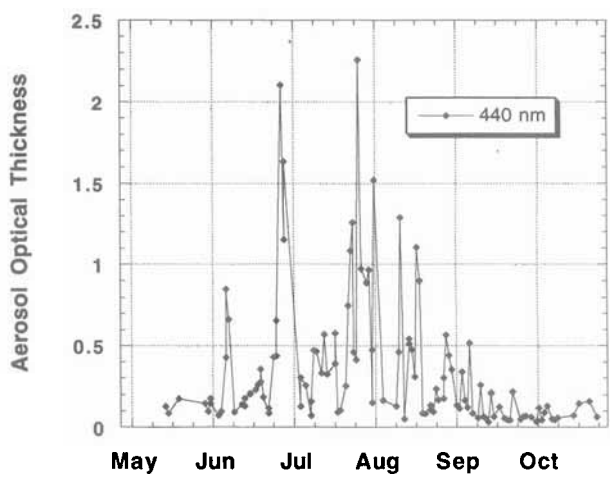

Figure 60.4 The seasonal dependence of the boreal forest daily averaged AOT (440 nm) measurements indicated several episodes of heavy aerosol loading in 1994, most of them lasting less than a week and interspersed with periods of very light aerosol loading. Data taken during this period are from north central Manatoba, Canada associated with the Boreal Ecosystem-Atmosphere Study (BOREAS).

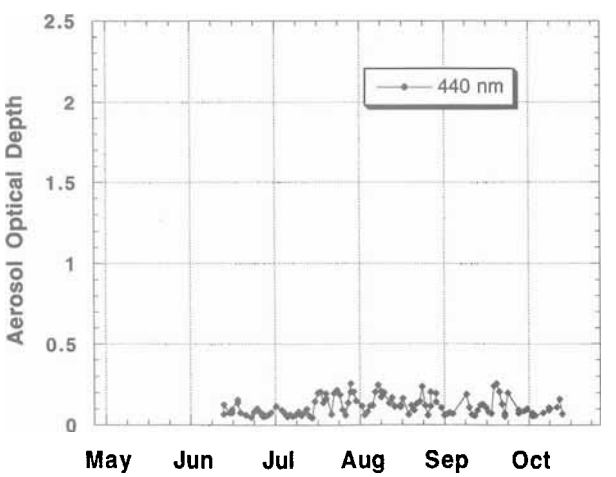

Figure 60.5 The seasonal trace of daily averaged AOT (440 nm) in the HJ Andrews experimental forest in the central Oregon Cascade mountains clearly shows a dry-season increase during July and August and parts of September. The magnitudes, however, are low and daily variations are likely to be due to advection of clean pacific air.

sources of emissions to increase the AOT during a time that could be called a burning season. Notice that the source of the emissions has not been documented and could be a mixture of biogenic aerosols, local industry (lumber mills), and automobile emissions, with wild and prescribed fires advected from the surrounding region. The almost daily cyclicity of the AOT in the burning season suggests that the emissions are highly localized and the concentration is greatly influenced by advection of clean Pacific air. The summer seasonal value of 0.13 at 440 nm, compared to 0.44 in the boreal forest and 0.61 in the Amazon, suggests that human influence in suppressing fires is profound in the mid-latitude forests and equally profound in the tropics for creating fires.

These data suggest that the anthropogenic influence on aerosol concentrations in the southern Amazon is significantly greater than wildfire aerosol sources in North America. Additionally, the Amazonian fire season appears more predictable as to time of emissions and concentrations. Thus, in the following sections, we focus on Amazonian aerosols to characterize the AOT, wavelength exponent, Pw, and size distribution for a cerrado site (Cuiaba), a forested site (Alta Floresta), and a nonburning region (Santarem) for each subseason. Statistics of the aerosol magnitudes and properties for each site may be found in Holben et al. (1995). Finally, at sites where two years of data are available, 1993 and 1994 are contrasted.

Cerrado Site-Cuiaba

Preburning Season

This period (9 June to 15 July 1993) almost certainly extended prior to our first measurements. The average aerosol optical thickness (AOT) and standard deviation (s.d.), was 0.18 ($\pm$0.06) at 440 nm and the Ångstrom wavelength exponent, α computed from 440 and 870 nm measurements, was 0.95 ($\pm$0.23) (table 60.1). The frequency distribution of the AOT_{440}, α and P_w illustrates the stability of the aerosol conditions and water vapor during this period (figure 60.6). These values are relatively typical for all sites during preburning and could be considered background levels that, in part, were influenced by the stratospheric Pinatubo aerosols during this time (Dutton 1994). The Pinatubo aerosol optical depth at 525 nm for this period was measured at mid-latitude sites (Rosen et al. 1994) to be $\sim$0.035 at a Northern Hemisphere site and 0.07 at a Southern Hemisphere site. The volume size distribution from the almucantar data typically shows a weak accumulation mode, a Pinatubo mode centered at 0.6 μm and a weak-coarse particle mode of about 8 μm, (figure 60.7). During very clear conditions ($AOT_{440} = 0.1$), the dominant mode is that caused by the Pinatubo aerosols. (In 1994, the Pinatubo mode was reduced in magnitude by half compared to 1993.) Measurements extended about 35 days at this level with very little diurnal variation and are likely to represent conditions in the dry season, prior to our measurements. They are also similar to the few measurements obtained during the wet season and therefore probably are good predictors of nonanthropogenic background conditions for the southern Amazon Basin.

Transition to Burning Season

A transition to the burning season occurs as a few agriculturists burn their fields before fuels in the region dry completely. A few fires emit a relatively small amount of aerosols into the atmosphere, resulting in small increases in the AOT. Because there is not widespread burning, the AOT drops back to near background levels until a few more fires are begun a few days later. This cyclical pattern may continue a few weeks. For Cuiaba in 1993, the transition season lasted for about three weeks (15 July to 6 August). The Ångstrom wavelength exponent (440/870 nm) during this time oscillated between the background levels of 0.9 to burning conditions of 1.6, with a mean of 1.31 (0.25 s.d.), and the AOT oscillated between background levels 0.18 and 0.9, with a mean of 0.38 (0.15 s.d.). Precipitable water remained low and fairly constant during this period, with the frequency distributed mainly between 2.0 and 3.0 cm and a mean of 2.4 cm.

Burning Season

During the nearly two-month burning portion of the dry season (7 August to 27 September), the AOT_{440} averaged 1.32 (0.46) with a wavelength exponent of 1.71 (0.12), indicating a large population of small particles for the two-month duration. AOT_{440} ranged from 0.40 to 2.80 for this period, but the wavelength exponent varied from 1.28 to 1.98; the larger number suggests the presence of fresher smoke due to a higher proportion of fine to large particles (figure 60.8*a* and 60.8*b*). Because most fires are ignited after local noon, a difference in the scattering and absorption properties would be expected between fresh smoke in the afternoon and aged smoke in the mornings. The difference between the morning and afternoon peak α frequency distributions shows only slight variations, from 1.7 and 1.8 in the morning and afternoon, respectively,

Table 60.1 Average AOT, s.d., and Pw during 1993 and 1994 dry seasons for Cuiaba, Alta Floresta, and Santarem

Location	λ (nm)	Preburn	Transition to burn	Burning	Transition to wet	Wet
Cuiaba, 1993	870	0.09 ± 0.02	0.15 ± 0.04	0.41 ± 0.13	0.15 ± 0.05	0.11 ± 0.04
	440	0.18 ± 0.06	0.38 ± 0.15	1.32 ± 0.46	0.37 ± 0.15	0.25 ± 0.08
	alpha	0.95 ± 0.23	1.31 ± 0.25	1.71 ± 0.12	1.25 ± 0.28	1.10 ± 0.17
Duration (days)		>35	21	50	~30	>90
	Pw (cm)	2.6 ± 0.5	2.4 ± 0.4	3.5 ± 0.7	4.0 ± 0.6	4.5 ± 0.5
Cuiaba, 1994	870	0.07 ± 0.02	0.20 ± 0.08	0.45 ± 0.15	NA	
	440	NA	NA	1.39 ± 0.51	NA	
	alpha	NA	NA	1.61 ± 0.17	NA	
Duration (days)		>30	~25	30	NA	
	Pw (cm)			3.4 ± 0.6		
Alta Floresta, 1993	870	0.10 ± 0.02	0.15 ± 0.06	0.42 ± 0.15	0.19 ± 0.05	0.15 ± 0.05
	440	0.19 ± 0.06	0.42 ± 0.27	1.34 ± 0.54	0.44 ± 0.14	0.35 ± 0.15
	alpha	0.86 ± 0.27	1.35 ± 0.31	1.69 ± 0.16	1.23 ± 0.22	1.16 ± 0.26
Duration (days)		60	~10	60	~30	
	Pw (cm)	2.9 ± 0.4	2.8 ± 0.4	4.0 ± 0.5	4.4 ± 0.3	5.0 ± 0.3
Alta Floresta, 1994	870	0.05 ± 0.01	0.11 ± 0.03	0.48 ± 0.17	0.20 ± 0.05	0.21 ± 0.08
	440	0.22 ± 0.07	0.60 ± 0.16	1.73 ± 0.62	0.54 ± 0.16	0.41 ± 0.18
	alpha	2.02 ± 0.41	2.49 ± 0.16	1.87 ± 0.00	1.48 ± 0.25	0.93 ± 0.23
Duration (days)		>60?	~15	>50	10	
	Pw (cm)	2.8 ± 0.3	2.8 ± 0.6	3.8 ± 1.0	4.4 ± 0.4	6.3 ± 0.4
Santarem, 1993	870	0.15 ± 0.05	NA	NA	0.23 ± 0.08	0.19 ± 0.07
	440	0.27 ± 0.09			0.44 ± 0.17	0.37 ± 0.17
	alpha	0.76 ± 0.21			0.94 ± 0.21	0.88 ± 0.28
Duration (days)		>35			~33	>45
	Pw (cm)	5.3 ± 1.0			5.8 ± 0.9	6.3 ± 0.4

and the distributions are fairly broad and nearly identical. The AOT_{440} frequency distributions also do not show a clear increase from morning to afternoon. Both situations suggest that the scenario of local burning around Cuiaba is less important and that much of the smoke is probably advected from surrounding regions.

Almucantar inversions at extremely high optical thicknesses were more difficult to obtain because of the inhomogenious distribution of the aerosols in the viewing scans of the instrument, as well as the instability induced when inverting multiple scattered radiation. Almucantars taken during average aerosol loading were often unsuccessfully inverted. Those which were inverted showed size distributions with very large accumulation modes, which masked the Pinatubo mode (figure 60.9). Typically, the accumulation mode was 20 times greater than background conditions, and the coarse-particle mode was approximately an order of magnitude above background conditions.

Precipitable water during this time increased from less than 2. cm early in August to more than 4. cm late in September (figure 60.8*c*). This rise would be expected to cause some variation in the aerosol properties, either directly by condensation or absorption, or indirectly by cloud processing. This change also suggests that cloud interaction with aerosols is likely to be more prevalent during the latter part of the burning season, and direct radiative forcing is more significant during the early part of the burning season. Contrasting the wavelength exponent between the first two weeks and the last two weeks in the burning season, however, does not indicate a significant difference between the properties of the aerosols in Cuiaba.

Transition to Wet Season

The transition to the wet season lasted from 27 September to 1 November and the wet season began thereafter, thus ending the widespread burning activity. Because data were scarce during these times, they were combined. The AOT_{440} frequency distribution is shifted toward small values typical of background conditions, but particulates from late-season burning account for the low percentage of larger AOTs. This shift is substantiated by the Ångstrom wavelength exponent which shows a wide distribution ranging from 0.9 for clear air to greater than 1.8 for smoke (figure 60.10*a*). The distribution of Pw is bimodal (figure 60.10*b*). The weaker mode (3. cm) reflects a few dry days during the transition, and the higher mode is more indicative of the wet season (4.7 cm). Few sky radiance data were taken during this time because of

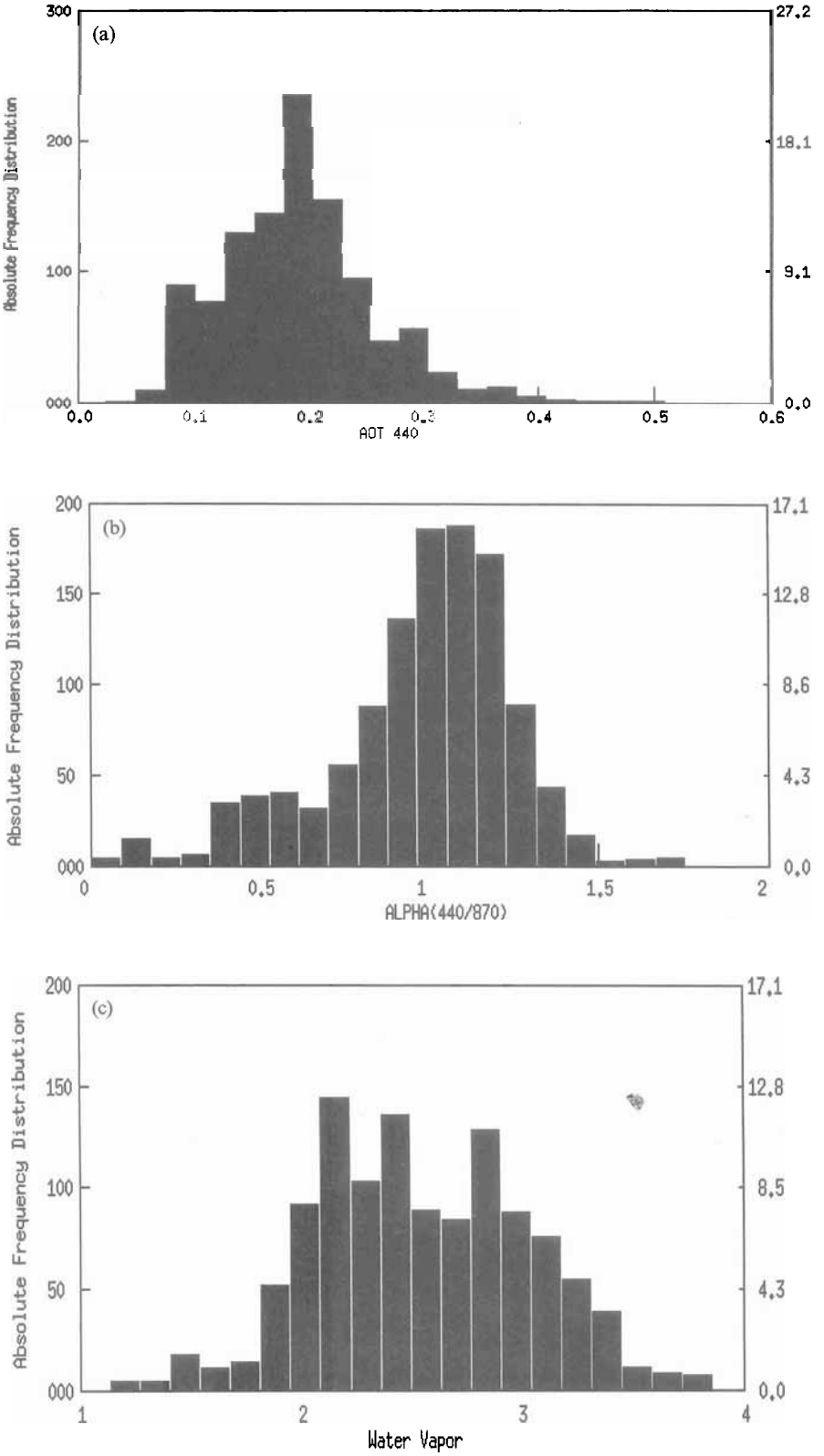

Figure 60.6 The frequency distribution of (*a*) AOT_{440}, (*b*) Ångstrom Wavelength Exponent (440/870), and (*c*) precipitable water (cm) indicate the temporal stability of the aerosol environment during the preburning season.

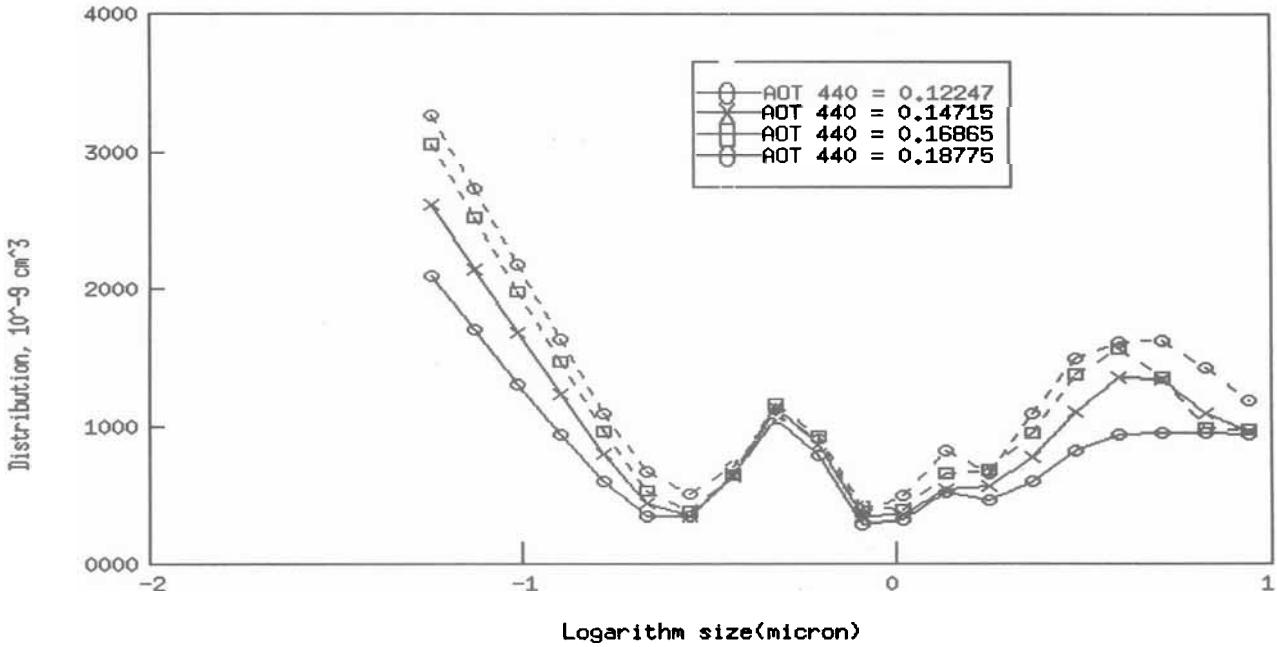

Figure 60.7 The size distribution during the preburning season showed a persistent mode centered at 0.6 μm, attributable to Pinatubo stratospheric aerosols and weak accumulation and coarse-particle modes during 1993.

increased clouds, and so climatological analysis of the size distribution was not possible.

Comparison to 1994

In 1994, the magnitudes of the averaged AOTs during both dry and burning seasons were very similar to 1993, but the duration was dramatically different for Cuiaba. For example, the transition to burning was essentially nonexistent in 1994, and the burning season began late in August and extended approximately 30 days, compared to 50 days in 1993. The timing and duration of the Pw remained approximately the same. The authors have no ancillary data to explain this observation.

Forested Site

Alta Floresta

Aerosol properties at forest sites where burning occurred were similar to those in the cerrado, the Ångstrom wavelength exponent was more variable during the burning season, probably due to greater influence of fresh smoke from local burning. An example is the Alta Floresta data record, where measurements began in June 1993 and ran through October. The data show a very clear preburning season ($AOT_{440} = 0.19$, $\alpha = 0.86$) until the transition in mid-July. The burning season began early in August ($AOT_{440} = 1.34$, $\alpha = 1.69$) with a duration of approximately 60 days (table 60.1). Compared to Cuiaba and the cerrado sites, these data show more distinction between morning and afternoon conditions with an increase in AOT and Ångstrom wavelength exponent in the afternoon (figure 60.11), but considering the entire burning season, these differences amount to an increase of only a few percent, and are likely to become significant only when individual cases are examined. The size distribution and phase function retrieved during this time also are very similar to conditions in Cuiaba. The size distributions indicated a close relationship to the AOTs; that is, low AOTs showed weaker accumulation and coarse-particle modes, and are entirely consistent with measurements in the cerrado (figures 60.12 and 60.7).

Considering the high AOT readings during he burning season and the variable meteorological conditions, it is fairly remarkable that biomass burning emissions of this magnitude are repeated each year. The burning season was reduced in 1994 to 50 days, but there was a substantial increase in the AOT_{440}, from 1.41 to 1.73 (table 60.1)

Santarem

In contrast, Santarem had no significant anthropogenic aerosol loading. The AOT_{440} remained at background

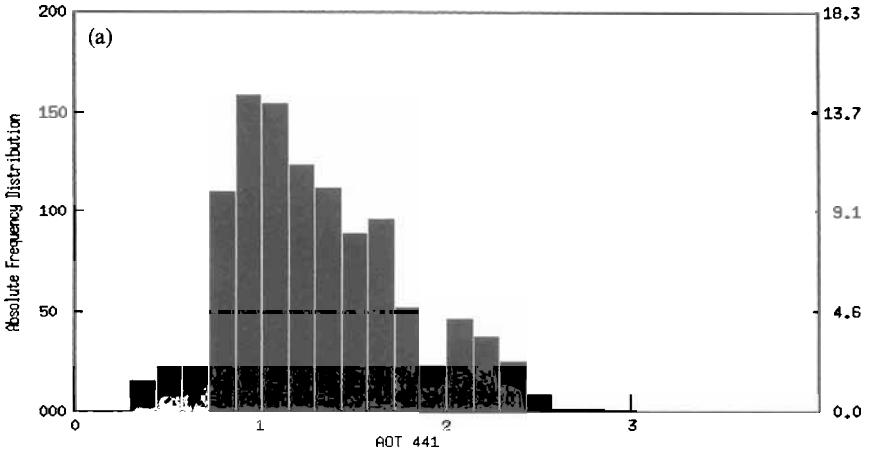

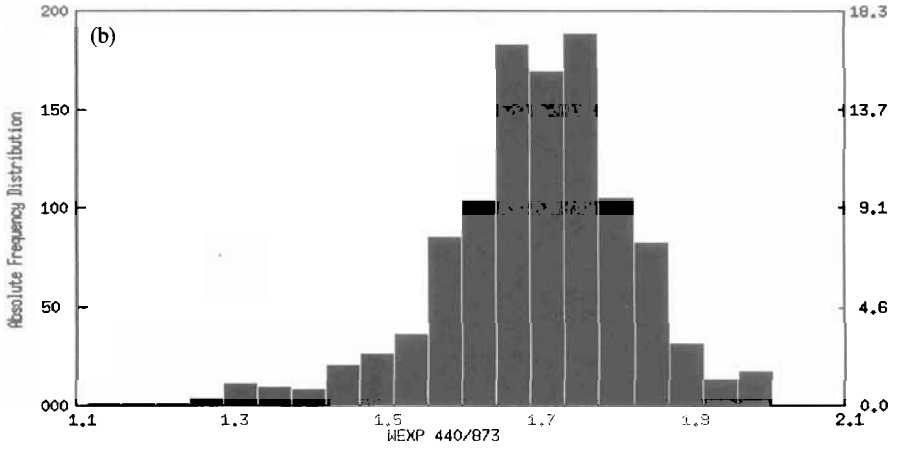

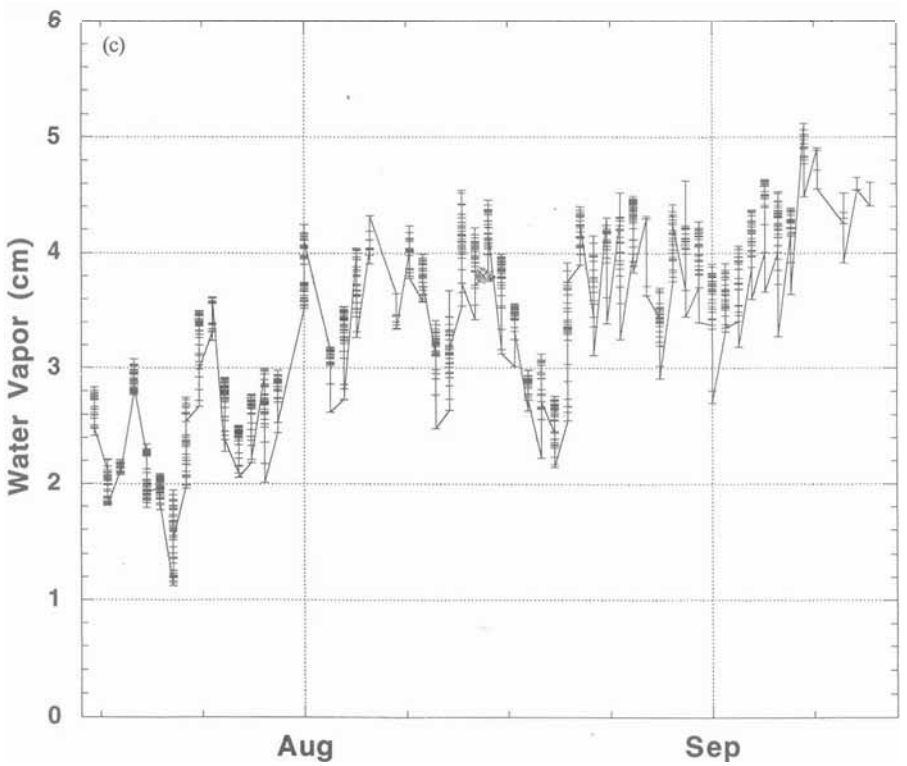

Figure 60.8 Analyzing the frequency distributions of the Burning season AOT_{440} (*a*) showed little variation when analyzed into morning and afternoon distributions. The burning-season frequency distribution of the Ångstrom wavelength exponent shows a slight bimodal distribution (*b*); the higher value is likely to represent a response to fresh smoke from afternoon fires. The Pw (*c*) during this period shows an increase from ~2.5 cm at the beginning of the burning period to ~4.0 cm near the end.

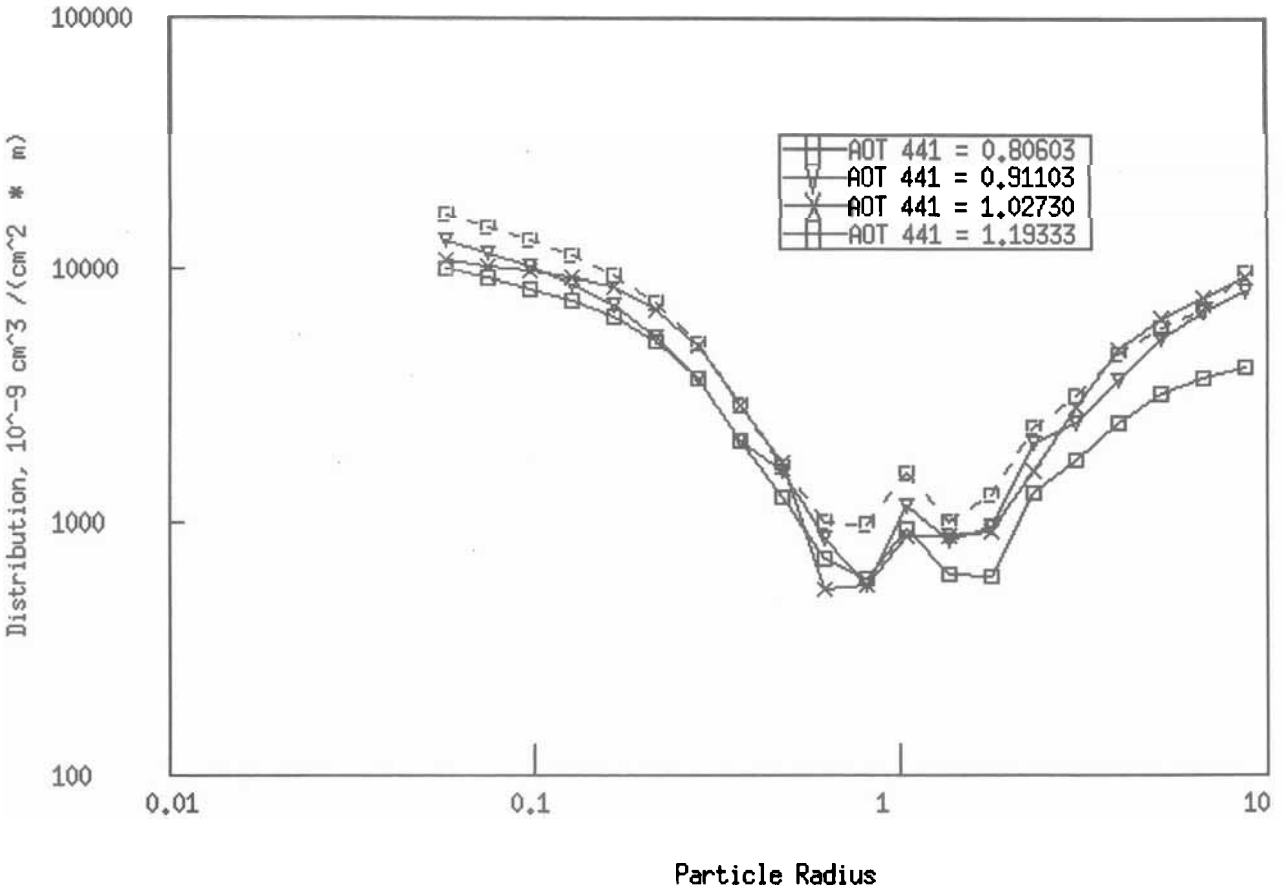

Figure 60.9 The size distribution during the burning season shows very large accumulation and coarse-particle modes based on retrievals from the almacantar measurements.

levels throughout the August and September dry season. The frequency distribution indicates that ~80% of the AOT_{440} is less than 0.2, and the wavelength exponent (0.88) is commensurate with what would be expected from combined background tropospheric and stratospheric Pinatubo aerosols (Rosen et al. 1994; Russell et al. 1993). Regional burning was reported ~100 km to the south, but the predominant wind direction is NE, where there are few sources of aerosols from biomass burning. There is a slight elevation of the AOT in November and December and a corresponding decrease in wavelength exponent. Since the Pw is highest during this time, thereby making the possibility of local or regional biomass burning sources unlikely, we suggest that the source may be Saharan dust transported across the Atlantic.

Seasonal, Diurnal, Temporal, and Spatial Variability

The variation in the AOT within the preburning subseason is very small and may be characterized by the simple s.d. (table 60.1). The burning season as well as the transition seasons show a great deal of variability in AOT (table 60.1), and the s.d. may not accurately represent the variation during this time because during the burning season two situations are common: (1) well-mixed uniform smoke is advected from regional fires, and (2) local fires cause great variability in the time-dependent aerosol concentration and properties.

The first case has two variants: In nonsource regions, aerosols are advected, creating aerosol fronts that result in large changes in aerosol concentrations in a time; in Jamari, the frontal boundaries are observed to be very active, in time resulting in large temporal variations in AOT, on the order of hours.

In sites within biomass burning regions, there are both diurnal variations in aerosol loading due to the diurnal cycle of the burning (Prins and Menzel 1994), and advection of smoke from adjacent burning regions. As an example, the AOT_{440} in Porto Nacional in one week (14 to 20 September, 1992) changed from strong diurnal increase in AOT each day from fires

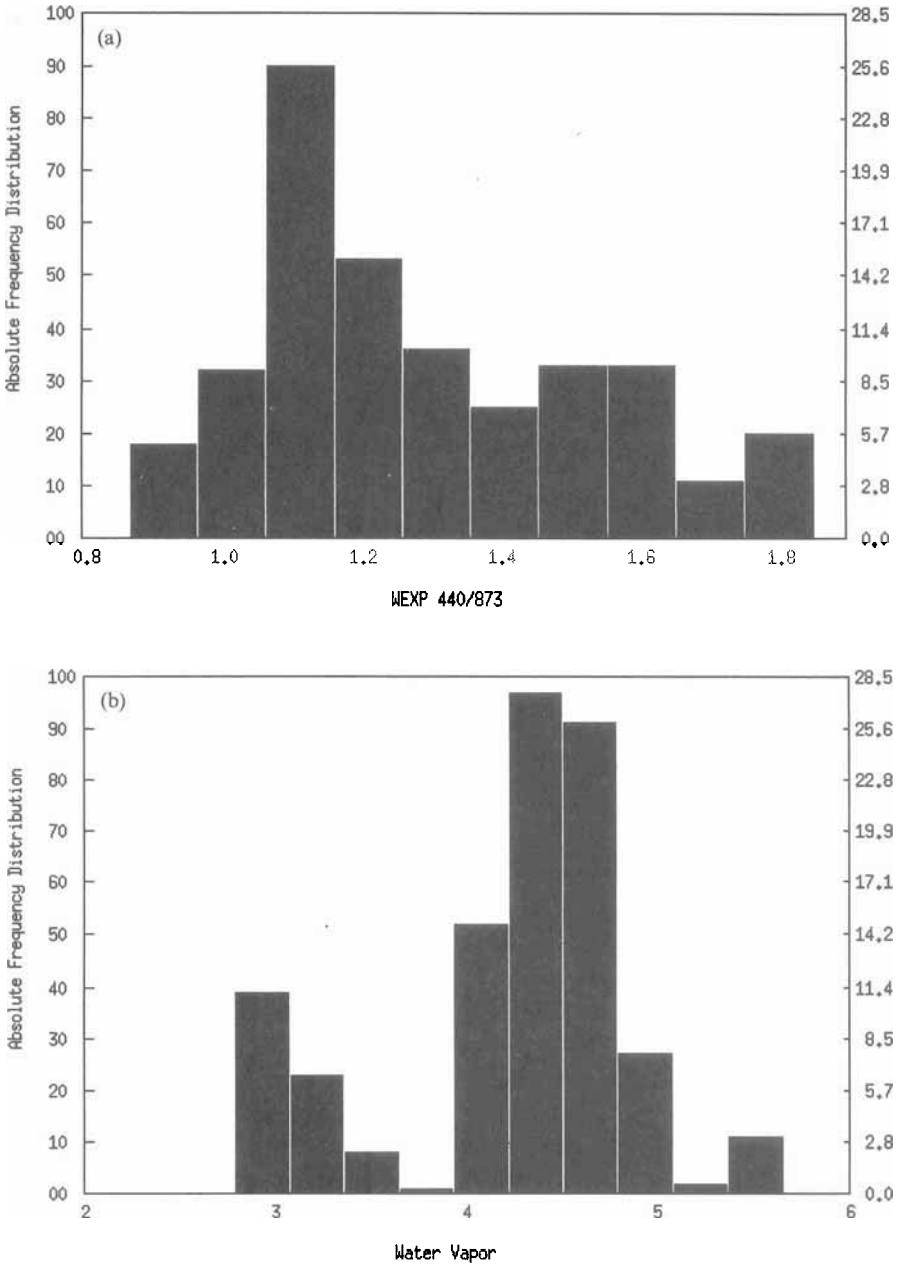

Figure 60.10 The wavelength exponent distribution (*a*) indicates a shift toward smaller values from the burning season and precipitable water (*b*) is a bimodal distribution indicating that water vapor is in transition during this time.

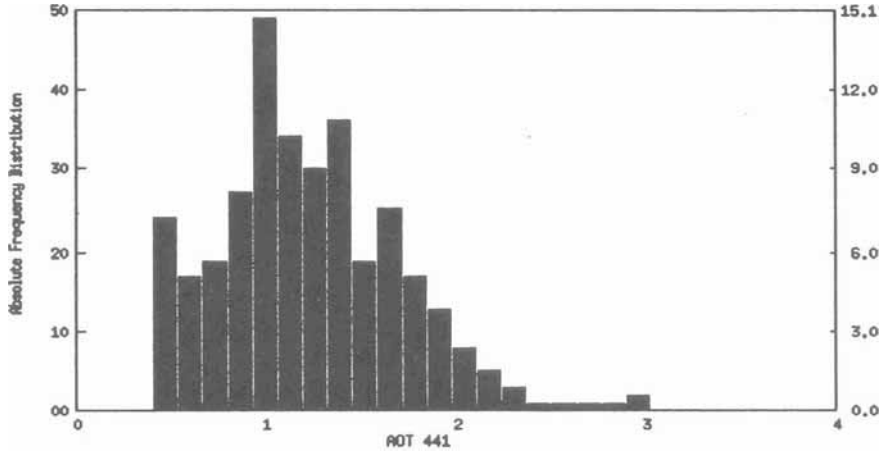

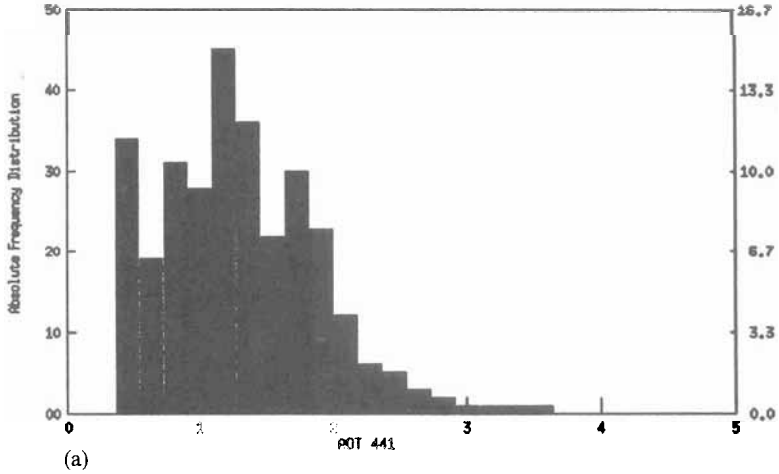

(a)

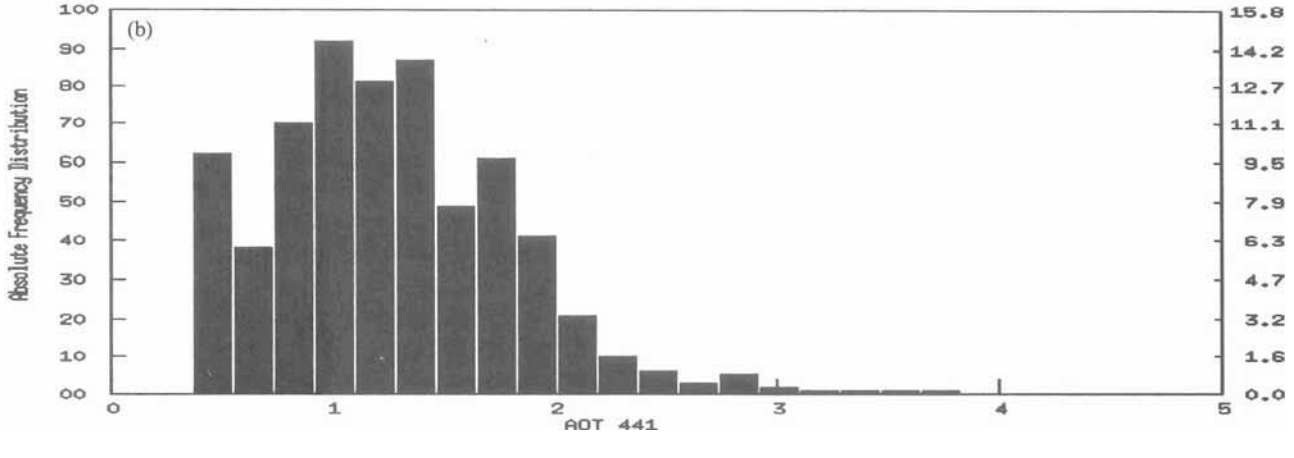

Figure 60.11 The frequency distributions for the Alta Floresta burning season AOTs (rows *a* and *b*) and alphas (*c* and *d*) were computed. Rows *a* and *c* show the morning and afternoon distributions (*left* and *right* respectively). Rows *b* and *d* are the distributions combined for the full day. Notice the slight afternoon shift to higher values in both the AOT and alpha distributions.

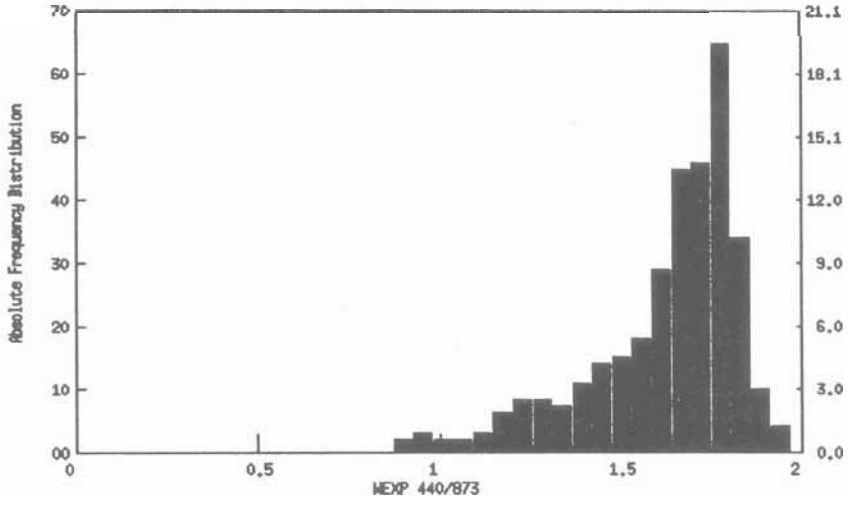

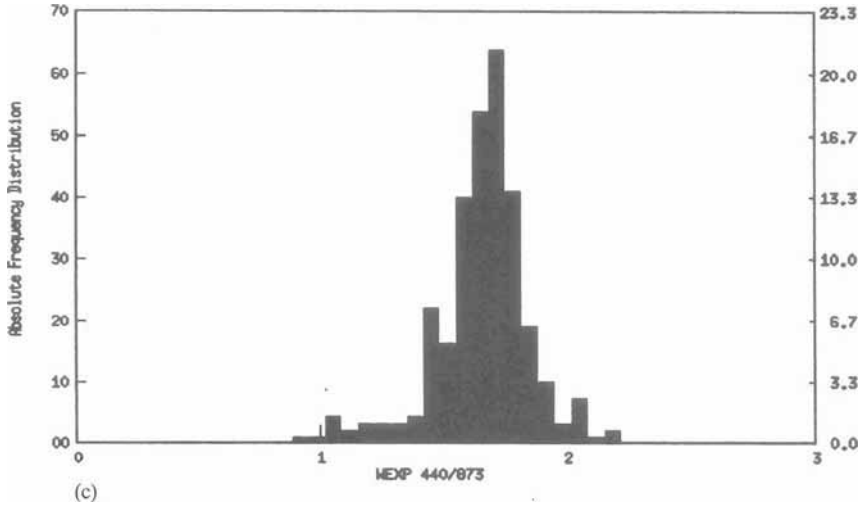

(c)

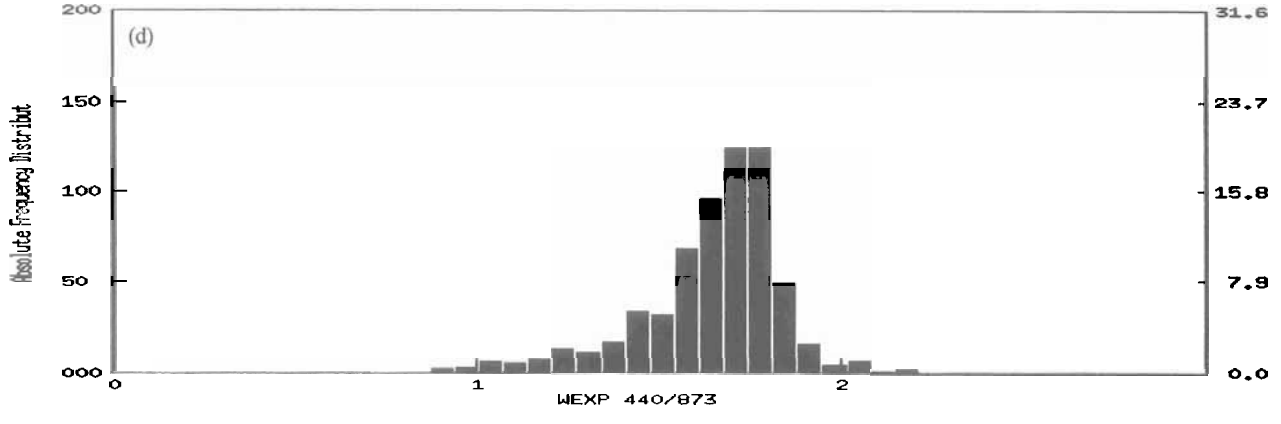

Figure 60.11 (continued)

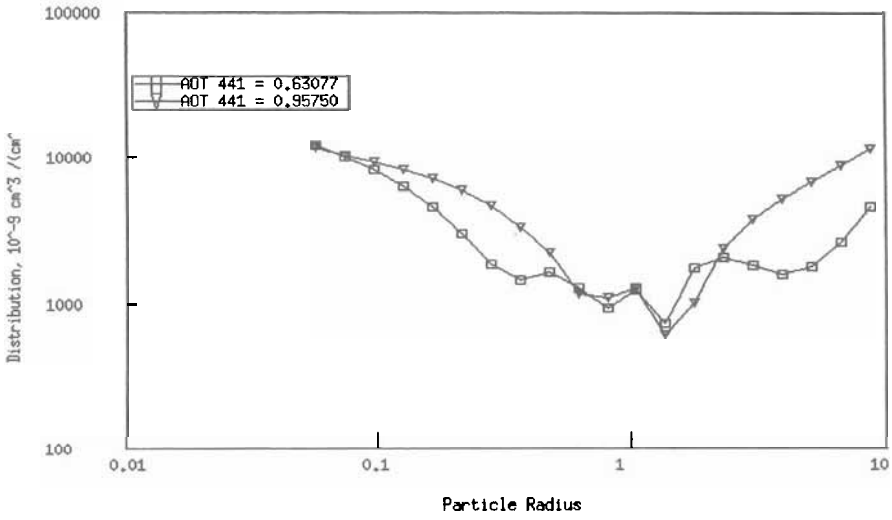

Figure 60.12 The retrieved size distribution shows an increase in the accumulation and coarse-particle modes with increasing AOT. The size distributions are similar to those retrieved from the cerrado.

starting in late morning to early afternoon, with the smoke aerosol dissipating by the next morning. The cycle would then begin again as fires were ignited by midday. But, then the meteorological conditions changed, and from 17 to 20 September, there were high AOT all day with no distinct diurnal variation (figure 60.13*a*). This condition resulted from advection of smoke from biomass burning areas within the region. Figures 60.13*b* and 60.13*c* show that for the same AOT_{440} from 1.1 to 1.7 the Ångstrom wavelength exponent was higher for the days that were dominated by smoke from local burning rather than the smoke that was advected into the area on 17 to 20 September, and was thus more aged. These data suggest smaller aerosol particles from the fresh smoke from fires burning on the same day rather than the more aged and regionally advected smoke. Thus, not only did the aerosol loading increase, but the properties of the aerosols changed as well. This behavior was commonly observed in the data at most sites simply because they were within burning regions away from local sources.

The second situation of intense local burning typically is represented by rapid oscillations in aerosol concentrations and properties, due to smoke from plume remnants not yet mixed in the atmosphere. The period of these events often is on the order of a few minutes to a few hours. Data from a transect along highway BR364 in Rondônia illustrates this phenomenon (figure 60.14). The stations that are farthest apart in this transect are only 90 km from each other. This placement typically occurs in the forested and forest converted areas, but is less common in the aerosol environment than in the regional events. Characterizing the aerosol properties from sky radiance measurements is nearly impossible during these events, whereas the spectral optical thickness is a reliable source of aerosol size distribution in these situations.

Discussion

The burning season for the Southern Hemisphere tropics and the Northern Hemisphere mid- and high latitudes occurs during the dry season, usually from May through September. Although observations in the mid-latitude forests were very limited, the aerosol concentrations throughout this period showed that aerosol loading is lightest in the highly managed mid-latitude forests, and at times is high for the boreal regions. Both regions exhibit highly variable conditions on a scale of a few days, which can vary from background aerosol loading to heavy aerosol loading depending on proximity to the fire. The southern Amazon clearly demonstrated the influence of anthropogenic fire sources on the aerosol loading for various widely separated sites. The duration and magnitude of the burning season are both longer and greater than the North American observations. The large cyclicity in the Northern Hemisphere aerosol concentrations is not present in the Southern Hemisphere, other than during the brief transition periods. This difference suggests a much larger number of fire sources and a reliable starting mechanism. Similar aerosol loading is less likely to occur at high latitudes, but exceptions can occur, as in the 1987 Chinese boreal forest fire (Cahoon et al. 1991).

The concentrations and optical properties of aerosols in the Amazon Basin have been shown to vary temporally and spatially due to emissions from an-

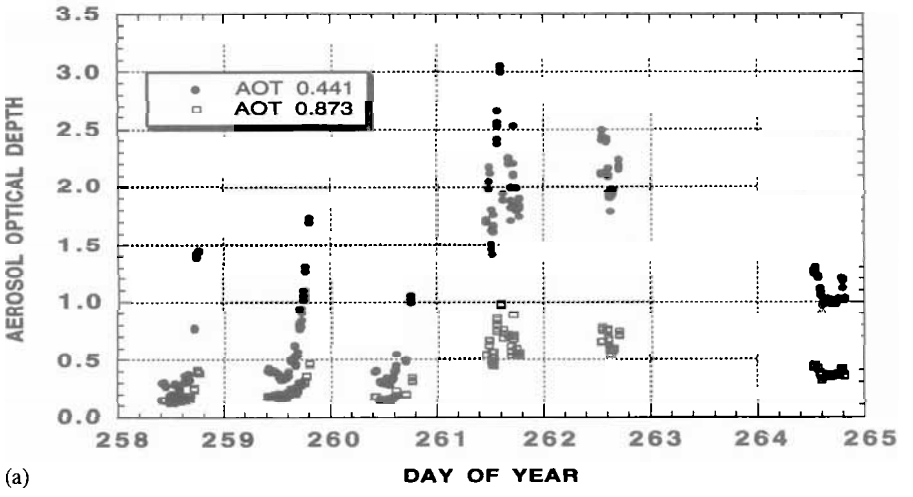

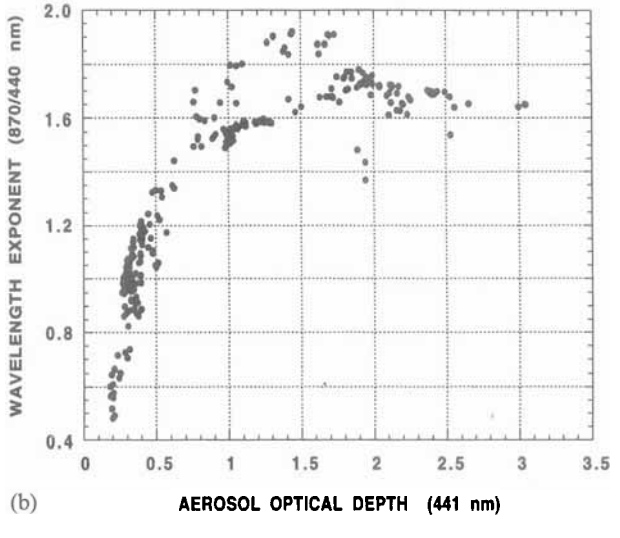

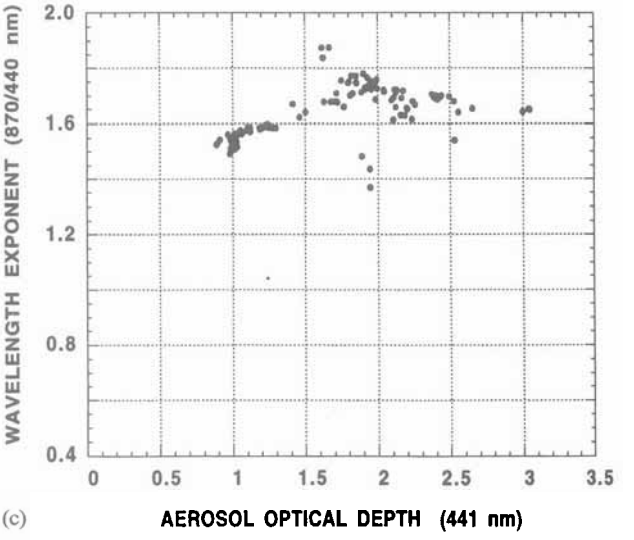

Figure 60.13 Seven days of AOT measurements in Porto Nacional show two regimes; (*a*) one in which local fires result in diurnal patterns of clear air and fresh smoke, and the other, in which smoke is advected from adjacent regions. The τ_{440} vs. α plot of this time series, (*b*), shows two distinct populations between the clean air (lower α) and the smoke-contaminated air (higher α). This apparent advection is a common influence for many of the sites. (*c*) is the same as (*b*) except for 17 to 20 September, when the wavelength exponent was less despite very high AOTs.

thropogenic biomass burning. Background aerosol concentrations ranged from 0.09 to 0.22 for AOT_{440} for all the southern Amazon measurement sites. Background levels were slightly modified in 1993 due to stratospheric Pinatubo aerosol loading; theses were particularly evident in the size distribution retrievals. However, by 1994 the volume distribution of the Pinatubo mode had been reduced by half. Due to lack of strong sources of anthropogenic aerosols, it is assumed that the majority of background aerosols are from natural biogenic sources.

The climatological dry season can last five months, but due to strong anthropogenic aerosol sources, we have defined four dry-season subseasons, including background, transition-to-burning, burning, and transition to wet season. Significant aerosol emissions are present during all but the preburning season. The transition seasons are characterized by a cycle of clear to smoky conditions, and the burning season by relatively constant and heavy aerosol loading. Ångstrom wavelength exponent measurements of fresh smoke (a day or less old) typically range from 1.8 to 2.2 (Kaufman et al. 1992, Holben et al. 1991). The histograms of the wavelength exponent during the burning season suggest that the smoke is typically aged more than one day. Cuiaba in 1993 and Alta Floresta in 1994 showed

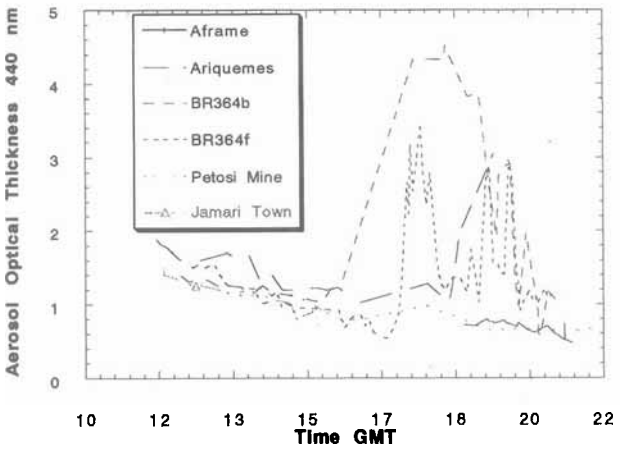

Figure 60.14 The AOT_{440} was measured throughout a day at sites various distances from local fires. Notice that until noon (1600 GMT) the AOT_{440} was very similar but diverted greatly in response to local fires. "Petosi Mine" and "Aframe" were located sufficiently far from active fires (~ 40 and 20 km respectively) that no influence was observed. Ariquemas and the BR364 sites were in some cases within a few km of local fires.

periods of four weeks or more of extremely high levels of aerosol loading from smoke advected from the surrounding region. The wavelength exponent during this time was typically 1.69 to 1.87, indicating that the smoke was aged (table 60.1).

Inversions of the sky radiances were relatively few; the AOT_{440} exceeded 1.0, thus the size distribution and phase function retrievals are biased and may not fully represent aerosol properties during heavy loading events. Given these limitations, size distributions indicated a significant Pinatubo mode in 1993 centered at 0.6 μm, which diminished by half in 1994. As the burning season advanced, the accumulation and coarse-particle modes increased, overwhelming the Pinatubo signal. In like manner, the retrieved phase function and asymmetry factor changed as the burning season advanced. For example, typical asymmetry factors in the preburning season were 0.70 @ 670 nm and decreased to 0.58 during the burning season. Further analysis of the retrieved phase function, computation of the hemispherical backscatter fraction (beta), and the radiative significance are discussed by Kaufman et al. (1995).

Precipitable water was shown to increase from a season low late in June through July to near wet season values in late September and early October. The increase ranged from approximately 50% to 100% of the dry-season minimum. This pattern held for all stations in the southern Amazon Basin and was particularly evident in Cuiaba. Average temperatures at the surface for the period increased only 2°C. Although relative humidity was not measured, the implication that it increased during this period corresponds to the time of most intense aerosol emissions from biomass burning. Despite this background, there has been no clear difference in size distributions, asymmetry factors, or wavelength exponents between early burning season and late burning season observations. This observation suggests that there is no growth in the aerosol size, even with the increase in available moisture, thus the Pw impact on optical properties of the aerosols is minor. Furthermore, the aerosol-Pw interaction appears to be minor compared to the direct effect of aerosol scattering and absorption on the surface radiation balance. Field campaigns are needed to verify these observations.

Acknowledgments

We thank Wayne Newcomb for the many days he spent on instrument details necessary for successful instrument network operations. Encouragement from Chris Justice and Yoram Kaufman has greatly facilitated development of a global network. Thanks to Diane Wickland and Tony Janetos for their confidence and financial support for the network concept. Special thanks to the many site managers in Brazil, and at the LTER and BOREAS sites, who have worked hard under difficult conditions for the last three years to collect these data. Also, we acknowledge the assistance of John Reagan for instrument evaluation and calibration and Didier Tanré for helping to develop the network. A big thanks to Dr. Ross Nelson for his valuable contributions in the field.

We also wish to express our appreciation to all the other participants who have embraced the open-data concept necessary for development, expansion, and inclusion of their data bases into a sun/sky radiometer global data base.

References

Artaxo, P., and C. Orsini. 1986. The emission of aerosol by plants, revealed by three receptor models. In G. Israel, ed., *Aerosols: Formation and Reactivity*, Pergamon, New York, pp. 148–151.

Artaxo, P., H. Storms, F. Bruynseels, R. Van Grieken, and W. Maenhaut. 1988. Composition and sources of aerosols from the Amazon Basin. *J. Geophys. Res.* 93, 1605–1615.

Artaxo, P., W. Maenhaut, H. Storms, and R. Van Grieken. 1990. Aerosol characteristics and sources for the Amazon Basin during the wet season. *J. Geophys. Res.* 95, 16971–16985.

Artaxo, P., F. Gerab, and M. L. C. Rabello, 1993c. Elemental composition of aerosol particles from two background monitoring sta-

tions in the Amazon Basin. *Nucl. Instr. Methods Phys. Res.* B75, 277–281.

Artaxo, P., F. Gerab, M. A. Yamasoe, and J. V. Martins. 1994. Fine mode aerosol composition at three long-term atmospheric monitoring sites in the Amazon Basin, *J. Geophys. Res.*, 99 (D11), 22 857–22 868.

Bird, R. E., and C. Riordan. 1986. Simple solar spectral model for direct and diffuse irradiance on horizontal and tilted planes at the Earth's surface for cloudless atmospheres. *J. Climate Appl. Meteor.* 25, 87–97.

Cachier, H., P. Buat-Menard, M. Fontugne, and J. Rancher. 1985. Source terms and source strengths of the carbonaceous aerosol in the tropics. *J. Atmos. Chem.* 3, 469–489.

Cahoon, Donald R., Jr., J. S. Levine, W. R. Cofer III, J. E. Miller, Patrick Minnis, G. M. Tennille, T. W. Yip, B. J. Stocks, and P. W. Heck. 1991. The great Chinese fire of 1987: A view from space. In Joel S. Levine, ed., *Global Biomass Burning: Atmospheric, Climatic and Biospheric Implications*, Cambridge, Mass. MIT Press, pp. 61–66.

Charlson, R. J., S. E. Schwartz, J. M. Hales, R. D. Cess, J. A. Coakley, Jr., J. E. Hansen, and D. J. Hofmann. 1992. Climate forcing by anthropogenic aerosols. *Science*, 255, 423–430.

Crutzen, P. J. and M. O. Andreae. 1990. Biomass burning in the tropics: Impact on atmospheric chemistry and biogeochemical cycles. *Science* 250, 1669–1678.

Dutton, E. G. 1994. Aerosol optical depth measurements from four NOAA/CMDL monitoring sites. In T. A. Boden, D. P. Kaiser, R. J. Sepanski, and F. W. Stoss, eds. *Trends '93: A Compendium of Data on Global Change*. ORNL/CDIAC-65. Carbon Dioxide Information Analysis Center, Oak Ridge National Laboratory, Oak Ridge, Tenn., pp. 484–494.

Halthore, R. N., Tom F. Eck, Brent N. Holben, and Brian L. Markham, 1996. Sunphotometric Measurements of Atmospheric Water Vapor Column Abundance in the 940-nm Band, in preparation.

Hanson, J. E. and A. A. Lacis. 1990. Sun and dust versus greenhouse gases: An assessment of their relative roles in global climate change. *Nature* 346, 713–719.

Harriss, R. C. 1990. The Amazon boundary layer experiment: Wet season 1987. *J. Geophys. Res.* 95, 16 721–16 736.

Holben, B. N., T. F. Eck, I. Slutsker, D. Tanré, J. P. Buis, A. Setzer, E. Vermote, J. Reagan, Y. Kaufman, T. Nakajima, F. Lavenu and I. Jankowiak, 1996. Automatic sun and sky scanning radiometer system for network aerosol monitoring, accepted by *RS of Environ.*

Holben, B. N., Y. J. Kaufman, A. Setzer, D. Tanre, and D. E. Ward. 1991. Optical properties of aerosol from biomass burning in the tropics, BASE-A. In Joel S. Levine, ed., *Global Biomass Burning*, Cambridge, Mass. MIT Press, pp. 403–411.

Holben B. N., A. Setzer, T. F. Eck, A. Pereira, I. Slutsker. 1995. Temporal and spatial variability of aerosol loading and properties during the Amazon Basin dry season, 1992–1994, submitted to *J. Geophys. Res.*

Kaufman, Y. J., A. Gitelson, A. Karnieli, E. Ganor, R. S. Fraser, T. Nakajima, S. Mattoo, and B. N. Holben. 1994. Size distribution and phase function of aerosol particles retrieved from sky brightness measurements, accepted by *JGR-Atmospheres.*

Kaufman, Y. J., A. Setzer, D. Ward, D. Tanré, B. N. Holben, P. Menzel, M. C. Pereira, and R. Rasmussen. 1992. Biomass burning airborne and spaceborne experiment in the Amazonas (BASE-A). *J. Geophy. Res.* 97, 14 581–14 599.

Kaufman, Y. J., and B. N. Holben. 1995. Backscattering by aerosol measurements for tropical biomass burning and eastern U.S. pollution, submitted to *J. Geophys. Res.*

Lawson, D. R., and J. W. Winchester. 1979. Atmospheric sulfur aerosol concentrations and characterisitics from the South American continent. *Science* 205, 1267–1269.

Nakajima, T., M. Tanaka, and T. Yamauchi. 1983. Retrieval of the optical properties of aerosols from aureole and extinction data. *Appl. Opt.* 22, 2951–2959.

Nakajima, T., T. Takamura, M. Yamano, M. Shiobara, T. Yamauchi, R. Goto, and K. Murai. 1986. Consistency of aerosol size distributions inferred from measurements of solar radiation and aerosols. *J. Meteor. Soc. Japan* 64, 765–776.

Nakajima, T. 1995. Personal communication.

Nimer, E. 1989. *Climatologia do Brasil*, IBGE, Rio de Janeiro.

Penner, J. E., R. J. Charlson, J. M. Hales, N. S. Laulainen, R. Leifer, T. Novakov, J. Ogren, L. F. Radke, S. E. Schwartz, and L. Travis. 1994. Quantifying and minimizing uncertainty of climate forcing by anthropogenic aerosols. *Bull Am. Meteor. Soc* 75(3), 375–399.

Penner, J. E., R. Dickinson, and C. O'Neill. 1992. Effects of aerosol from biomass burning on the global radiation budget. *Science* 256, 1432–1434.

Prins, E. M., and W. P. Menzel. 1994. Trends in South American biomass burning detected with the GOES visible infrared spin scan radiometer atmospheric sounder from 1983 to 1991. *JGR* 99(D8) 16 719–16 735.

Prins, E. M., and W. P. Menzel. 1992. Geostationary satellite detection of biomass burning in South America. *Int. J. Remote Sensing* 13(15), 2783–2799.

Remer, L. A., Y. Kaufman, and B. Holben. 1995. Comparison of smoke aerosol and urban/industrial aerosol optical properties. Paper presented at the Chapman Conference Proceedings, 13–17 March, Williamsburg, Va.

Setzer, A., and M. C. Pereira. 1991. Amazonia biomass burning in 1987 and an estimate of their tropospheric emissions. *Ambio* 20, 19–22.

Skoke, D., and C. Tucker. 1993. Tropical deforestation and habitat fragmentation in the Amazon: Satellite data from 1978 to 1988. *Science* 260, 1905–1909.

Stocks, B. J. 1991. The extent and impact of forest fires in northern circumpolar countries. In Joel S. Levine. ed., *Global Biomass Burning: Atmospheric, Climatic and Biospheric Implications*, Cambridge, Mass., MIT Press., pp. 197–201.

Ward, D. E., and C. C. Hardy. 1991. Smoke emissions from wildland fires. *Environ. Int.* 17, 117–134.